Aqueous Solution of Ketone Solvent for Enhanced Water Imbibition in Fractured Carbonate Reservoirs

Mingyuan Wang, Gayan A. Abeykoon, Francisco J. Argüelles-Vivas, and **Ryosuke Okuno,**
University of Texas at Austin

Summary

This paper presents four dynamic imbibition experiments using fractured limestone cores with aqueous solutions of 3-pentanone and a nonionic surfactant. Results of the dynamic imbibition experiments were analyzed by the material balance for components: oil, brine, and chemical (3-pentanone or surfactant). The analysis resulted in a quantitative evaluation of the imbibed fraction of the injected components (brine and chemical additives) and the relative contribution of these components to the oil displacement in the matrix.

Results show that 3-pentanone and surfactant both can enhance the imbibition of brine through wettability alteration; however, 3-pentanone is more efficient in transferring from a fracture to the surrounding matrix. The imbibed fraction was more than 57.0% for 3-pentanone, and only 6.0% for surfactant at the end of the chemical-slug stage. During injection of the 3-pentanone solution, brine and 3-pentanone both displaced oil from the matrix pore volume (PV).

Results of the material-balance analysis suggest that an optimal process with an aqueous wettability modifier will have a large imbibed fraction to rapidly enhance the oil displacement by brine in the matrix. Such a process will benefit from chase brine and soaking (or shut-in) so that the oil recovery can be maximized for a small amount of chemical injection.

Introduction

Carbonate reservoirs are often naturally fractured and characterized to be oil-wet or mixed-wet (Roehl and Choquette 1985). Negative capillary pressure tends to hinder brine imbibition from fractures into the surrounding matrices, resulting in low waterflood recovery in carbonate reservoirs (Allan and Sun 2003). Various methods have been studied for enhancing oil recovery from such reservoirs, such as surfactant-solution injection, alcohol-solution injection, and low-salinity-water injection (Hirasaki and Zhang 2004; Adibhatla and Mohanty 2008b; Austad et al. 2008; Gupta and Mohanty 2011; Parra et al. 2016; Li et al. 2017; Lu et al. 2019).

For surfactant injection, cationic, anionic, and nonionic surfactants have been tested to enhance oil recovery from oil-wet carbonate rocks. Austad and Milter (1997) showed that cationic surfactants could enhance water imbibition into oil-wet chalk through wettability alteration. Adibhatla and Mohanty (2008b) and Gupta and Mohanty (2010) demonstrated that anionic and nonionic surfactant solutions yielded high oil recovery [60% original oil in place (OOIP)] from oil-wet carbonate cores. Wettability alteration and/or interfacial-tension (IFT) reduction between the oleic and aqueous phases are the main mechanisms of enhanced oil recovery from oil-wet carbonate by surfactant solutions (Gupta and Mohanty 2011; Mirzaei et al. 2016). Adibhatla and Mohanty (2008a) showed that when surfactants altered the wettability to a water-wet state, the oil-recovery rate increased with increasing IFT. This was because the capillary pressure gradient increased with IFT, which induced countercurrent imbibition. When surfactants did not significantly alter the wettability, efficient oil recovery was achieved with lower IFT systems (Adibhatla and Mohanty 2008a). As IFT was reduced, the buoyant force exceeded the capillary force, resulting in oil recovery by gravity drainage (Adibhatla and Mohanty 2008a). Several studies also indicated that the imbibition rate was controlled by the surfactant diffusivity, which was an important parameter that controlled the oil recovery (Mirzaei and DiCarlo 2013).

Besides capillary and buoyant forces, several studies showed that viscous force was also important in enhanced oil recovery from fractured oil-wet carbonate rocks (Parra et al. 2016; Mejia 2018). A simulation study by Abbasi et al. (2010) indicated that a small viscous transverse-pressure gradient could enhance surfactant imbibition from the fracture into the matrix. Parra et al. (2016) performed dynamic imbibition experiments and demonstrated that viscous microemulsion created by the surfactant formulation could induce transverse-pressure gradients to enhance the water imbibition.

The 1-pentanol solution was recently proposed for the wettability alteration of calcite by Lu et al. (2019). Their experiments showed that the contact angle of crude oil on the calcite surface was significantly reduced with a 1 wt% 1-pentanol solution. A possible mechanism is that 1-pentanol increased the thickness of a thin brine film between oil and the surface.

Low-salinity-water injection has also been studied for improving oil recovery in carbonate reservoirs. A mechanism of wettability alteration by seawater was proposed by Austad et al. (2008). The adsorbed carboxylic groups on chalk can be removed through synergistic interactions of Ca^{2+}, Mg^{2+}, and SO_4^{2-} ions, resulting in wettability alteration of chalk surface. This mechanism depends on the polar/polar interaction between the chalk surface and sulfate ions.

Recently, 3-pentanone was investigated as an additive to reservoir brine (RB) for enhanced water imbibition into mixed- or oil-wet matrices (Wang et al. 2019a). The symmetric dialkyl ketone of 3-pentanone is a colorless liquid at standard conditions, and is commercially available at a relatively low cost. It is identified in various foods, such as guava fruit, kiwi fruit, musk strawberries, and olive oils (Idstein and Schreier 1985; Bartley and Schwede 1989; Nishimura et al. 1989; Cavalli et al. 2004; Berlioz et al. 2006; Pet'ka et al. 2012). It is also used in vitamin synthesis (Baglai et al. 1988). The ability of 3-pentanone to alter rock wettability was demonstrated by two sets of imbibition experiments with RB and a 1.1 wt% 3-pentanone solution (3pRB) (Wang et al. 2019a). The experiments were performed with oil-aged Indiana Limestone cores at 347 K. The Amott index to water was calculated to be 0.23 for the RB case and 0.76 for the 3pRB case. The wettability alteration by the 3-pentanone was caused by the dipole-ion interaction between the 3-pentanone's carbonyl oxygen and the positively charged rock surface, which reduced the polar/polar interaction between oil

Original SPE manuscript received for review 26 March 2020. Revised manuscript received for review 12 July 2020. Paper (SPE 200340) peer approved 17 July 2020.

molecules and the calcite surface. In addition to wettability alteration, 3-pentanone is miscible with oil, resulting in oil displacement by 3-pentanone through oil swelling and oil-viscosity reduction.

Wang et al. (2019b) compared 3-pentanone with a nonionic surfactant for enhancing water imbibition from a fracture into the surrounding matrix. The surfactant used was 2-ethylhexanol-4 propylene oxide-15 ethylene oxide (2-EH-4PO-15EO). Two sets of dynamic imbibition experiments were compared using fractured limestone cores with 1.1 wt% 3pRB and a 1 wt% surfactant solution at 347 K. The oil recovery of the 3-pentanone case was more rapid than that of the surfactant case. The main reason is that 3-pentanone did not affect the IFT between the oleic and aqueous phases, but the surfactant decreased the IFT by two orders of magnitude.

Previous results showed that 3-pentanone is a promising wettability modifier for enhancing brine imbibition from a fracture to the surrounding matrix. The oil recovery during this process depends on the mass transfer of components between the fracture and the matrix. The injected 3-pentanone is first imbibed into the matrix to change rock wettability; then, the brine is imbibed into the matrix. As a result, the oil is displaced by both the imbibed brine and 3-pentanone from the matrix to the fracture. Therefore, the quantification of the mass transfer of components between the fracture and the matrix is crucial to understand the underlying physics during the enhanced brine-imbibition process. For example, it is unknown how much of the injected chemical [e.g., surfactant and 3-pentanone in Wang et al. (2019b)] is imbibed from a fracture into the surrounding matrix. Also, the relative contribution of brine and 3-pentanone to displacing oil from the matrix PV is unknown. Such fundamental information is commonly important for the application of wettability modifiers in fractured reservoirs and necessary for finding operational strategies (e.g., chase-brine injection and the shut-in period during huff 'n' puff operation).

Wettability alteration is commonly studied by spontaneous imbibition using an Amott cell. Although simple, this conventional method does not provide details of mass transfer between the fracture and matrix during the experiment. Also, experimental conditions are usually limited by the Amott cell. Researchers recently used computed tomography (CT) scan to monitor spontaneous-imbibition experiments (Alvarez et al. 2014, 2018a, 2018b; Mirzaei et al. 2016; Alvarez and Schechter 2017). The CT scanner measures the density of the material placed inside the scanner (Mirzaei et al. 2016). The color-coded relative-density images of the core can be used to dynamically visualize the spontaneous imbibition (Alvarez et al. 2018a). The density data from the CT scan were also reported as the CT number (Mirzaei et al. 2016). Porosity, water/oil saturation, and imbibition-front position can be calculated from the CT number (Mirzaei et al. 2016). The CT scan provides valuable information about the underlying physics during spontaneous imbibition. In this research, we took a more-traditional approach using material balance during coreflooding. We show a detailed analysis of components' flow during dynamic imbibition using a fractured core. This research method is the main novelty in this paper, which turned out to be quite useful for answering the questions described previously.

In the next section, the experimental methods and material-balance formulation are presented. The section Experimental Results presents the main results from the experiments and material-balance analysis. The section Discussion discusses the results from the experiments and the material-balance analysis. We end with the section Conclusions.

Methods of Experiments and Material-Balance Analysis

This section presents the methods of experiments and material-balance analysis for this study. The main experimental data are obtained through three sets of dynamic imbibition experiments with 1.1 wt% 3pRB and one set with 1.0 wt% surfactant solution in RB at 347 K.

Reservoir-Fluid Properties. The crude oil used in this research is from a tight oil reservoir in Texas. The reservoir temperature is 347 K. The crude-oil properties and RB composition are shown in **Tables 1 and 2** (Wang et al. 2019a). The RB density and viscosity are 1030 kg/m^3 and 0.56 cp, respectively, at reservoir temperature and atmospheric pressure (Wang et al. 2019a). The oil densities and viscosities measured at different conditions are shown in **Figs. 1 and 2** (Wang et al. 2019a). The crude-oil/RB IFT is 11.44 mN/m at reservoir temperature and atmospheric pressure (Wang et al. 2019a).

Molecular weight (g/mol)		186
Density (kg/m^3)		823 (at 289 K)
		780 (at 347 K)
SARA (wt%)	Saturates	76.7
	Aromatics	20.1
	Resins	3.2
	Asphaltenes (pentane insoluble)	<0.1

Table 1—Properties of the crude-oil sample used in this research. Oil densities and viscosities at high pressures are presented in Figs. 1 and 2 (Wang et al. 2019a). SARA = saturates/aromatics/resins/asphaltenes.

Cations	ppm	Anions	ppm
Na^+	25,170	Cl^-	41,756
K^+	210	SO_4^{2-}	108
Ca^{2+}	1,292	–	–
Mg^{2+}	187	–	–

Table 2—Composition of the RB used in this research (68,722 ppm). The density of RB was measured to be 1030 kg/m^3 at 347 K and atmospheric pressure (Wang et al. 2019a).

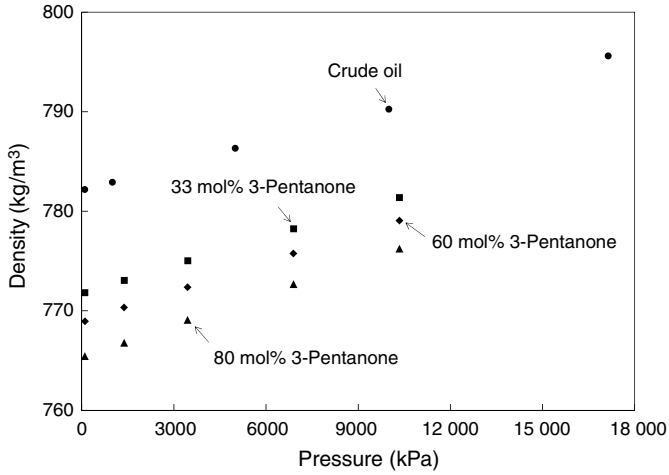

Fig. 1—Densities of crude oil and its mixtures with 3-pentanone. The crude-oil densities were measured at 344 K. All other densities were measured at 347 K (Wang et al. 2019a).

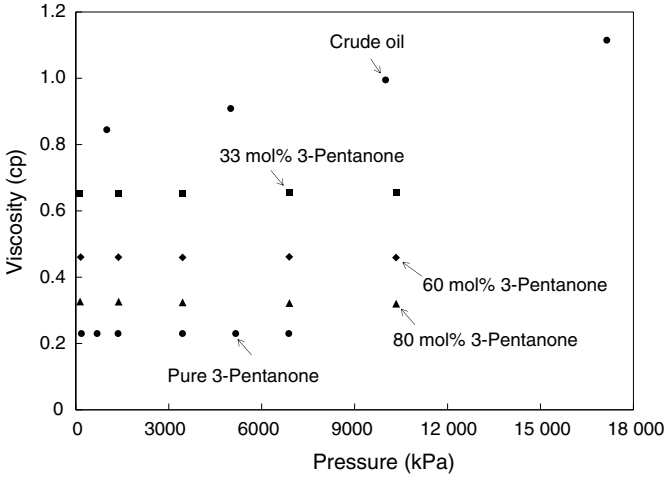

Fig. 2—Viscosities of crude oil and its mixtures with 3-pentanone. The crude-oil viscosities were measured at 344 K and the other viscosities were measured at 347 K (Wang et al. 2019a).

3-Pentanone Properties. The purity of 3-pentanone (Sigma-Aldrich) used in this research was higher than 99%. The density of 3-pentanone is 760 kg/m^3 at reservoir temperature and atmospheric pressure (Daubert and Danner 1985). Contact-angle experiments and IFT experiments by Wang et al. (2019a) showed that 3-pentanone rapidly changed the wettability of calcite from oil-wet to strongly water-wet without affecting the IFT between the aqueous and oleic phases. Also, 3-pentanone can dilute crude oil as a solvent, which was demonstrated by density and viscosity experiments for mixtures of crude oil with 3-pentanone (Figs. 1 and 2) (Wang et al. 2019a). The viscosity of the mixtures changed slightly with pressure. This is partly because 3-pentanone viscosity is weakly sensitive to pressure. In this research, the viscosity of 3-pentanone was measured to be 0.23 cp at 347 K and pressures from 178 to 6873 kPa. Besides 3-pentanone, Bhide et al. (2003) presented that viscosities of dimethyl ether, another oxygenated solvent, were weakly correlated with pressure. The viscosity behavior of these oxygenated solvents is quite different from that of *n*-alkanes. For example, *n*-heptane is close to 3-pentanone in terms of volatility, but its viscosity increases by 9.5% when the pressure increases from 178 to 6873 kPa at 347 K.

The solubility limit of 3-pentanone in RB at reservoir temperature was measured to be 1.1 wt%, which defines the 3-pentanone concentration in RB used in this research (Wang et al. 2019a). The 1.1 wt% 3pRB density is 1030 kg/m^3 at reservoir temperature and atmospheric pressure (Wang et al. 2019a). The densities of RB and 1.1 wt% 3pRB were measured to be the same at 347 K and atmospheric pressure likely because of the volume change on mixing of 3-pentanone and RB. When 3-pentanone is mixed with RB, there is a small shrinkage in the total volume. Therefore, the measured density value for the mixture is higher than the one based on the ideal mixing.

The data in the literature show the volume change on mixing of 3-pentanone and water. Ramanjappa and Rajagopal (1988) reported densities of the 3-pentanone/water mixtures at different temperatures and atmospheric pressure. The volume change on mixing of 3-pentanone and water was found to be between –0.16 and –0.27% when the 3-pentanone concentration was between 0.8 and 1.5 wt%. The volume change on mixing reported in this research is comparable with the data in the literature, as will be discussed in the subsection Material Balance for a Fractured Core.

Surfactant Formulation. A nonionic surfactant with ultrashort hydrophobe, 2-EH-4PO-15EO, was used in this research (Wang et al. 2019b). It was made by alkoxylation of 2-ethylhexanol with four propylene oxide and 15 ethylene oxide groups (Harcros Chemicals). The propylene oxide group affects the hydrophobicity of the surfactant, and the ethylene oxide group affects the aqueous stability. The concentration of 2-EH-4PO-15EO in RB used in this research was 1 wt% (Wang et al. 2019b).

The surfactant solution changed the contact angle from 134 to 47° within 1 day, which demonstrated that 2-EH-4PO-15EO and 3-pentanone were comparable as wettability modifiers (Wang et al. 2019b). The IFT between the crude oil and the 2-EH-4PO-15EO solution was measured to be 0.21 mN/m at reservoir temperature and atmospheric pressure (Wang et al. 2019b).

Experimental Procedure for Dynamic Imbibition. A total of four dynamic imbibition experiments were performed at 347 K with fractured limestone cores. Two of them were performed in a vertically upward direction, and the others horizontally. This subsection describes the procedure for the horizontal dynamic imbibition, which largely follows the procedure presented in Wang et al. (2019b) for the vertical experiments. The properties of the Indiana Limestone cores and the injection scheme for four dynamic imbibitions are also summarized in this section.

The dimensions of the Indiana Limestone cores were 0.0254 m in diameter and 0.127 m in length (Wang et al. 2019b). The cores were first saturated with RB and then crude oil. Porosities, permeabilities, and water and oil saturations of the cores were measured during this process. The cores were then aged in the crude oil for more than 4 months at reservoir temperature. For the two cores for vertical dynamic imbibition, oilflooding after this long aging period resulted in undetectable water production; therefore, the two cores for horizontal dynamic imbibition were not flooded by oil after the oil aging.

Each core was cut by an electric saw along the longitudinal axis to create an artificial fracture. During the cutting process, water or oil was not applied on the cutting blade to avoid an undesirable change of the saturation distribution inside the core. The fracture aperture was maintained by polytetrafluoroethylene (PTFE) spacers with 0.001 m in width and 0.127 m in length (Mejia 2018). Then, the core halves and the PTFE spacers in the fracture were wrapped with a PTFE tube and placed inside a horizontally oriented core holder, with the fracture being vertically oriented. **Table 3** summarizes the properties of the fractured cores. Ghosh and Mohanty (2019) and Boukadi et al. (1994) reported similar initial water/oil saturations with Indiana Limestone cores. The samples used in Boukadi et al. (1994) have similar porosity and permeability as the samples used in this study.

	Core 1	Core 2	Core 3	Core 4
Matrix porosity	0.197	0.203	0.175	0.215
Matrix permeability (md)	30.8	41.4	13.0	34.9
Matrix water saturation	0.506	0.596	0.540	0.620
Matrix oil saturation	0.494	0.404	0.460	0.380
Mass of the core before cutting (kg)	0.14847	0.14777	0.15063	0.14839
Mass of the core after cutting (kg)	0.13691	0.13622	0.13952	0.13726
Matrix PV after cutting (m^3)	1.166×10^{-5}	1.202×10^{-5}	1.043×10^{-5}	1.279×10^{-5}
Pressure drop along with the core (kPa)	6.688 (at 900 cm^3/h)	6.964 (at 900 cm^3/h)	7.308 (at 500 cm^3/h)	5.861 (at 500 cm^3/h)
Overburden pressure (kPa)	4137	6274	689	1724
Fracture aperture (m)	1.215×10^{-4}	1.199×10^{-4}	0.970×10^{-4}	1.044×10^{-4}
Fracture permeability (darcies)	1246	1214	795	913
Permeability contrast between fracture and matrix	40455	29324	61154	26160
Flow capacity of fracture (m^3)	1.494×10^{-13}	1.437×10^{-13}	7.610×10^{-14}	9.407×10^{-14}
Fracture volume (m^3)	3.920×10^{-7}	3.870×10^{-7}	3.129×10^{-7}	3.368×10^{-7}
Fracture volume and matrix PV (m^3)	1.205×10^{-5}	1.241×10^{-5}	1.074×10^{-5}	1.313×10^{-5}

Table 3—Properties of the cores used for coreflooding experiments. Core 1 was used for vertical dynamic imbibition with 1.1 wt% 3pRB. Core 2 was used for vertical dynamic imbibition with 1.0 wt% 2-EH-4PO-15EO solution in RB (Wang et al. 2019b). Core 3 was used for horizontal dynamic imbibition with 1.1 wt% 3pRB. Core 4 was used for horizontal dynamic imbibition with 1.1 wt% 3pRB.

Fig. 3 shows the experimental setup for horizontal dynamic imbibition. It consisted of accumulators for crude oil, RB, and chemical solution (3-pentanone/surfactant), a pump, a Hassler-type core-holder, a hydraulic manual pump to keep the overburden pressure of the core holder, a pressure gauge, graduating cylinders, and an oven. The experiments were performed at reservoir temperature. The crude oil was injected into the core first to displace any gas inside the fracture and quantify the fracture permeability at 500 cm^3/h under an overburden pressure (Wang et al. 2019b). Table 3 provides the pressure drops along with the corresponding flow rates and the overburden pressures used.

Fracture apertures and fracture permeabilities were quantified using the method provided by Mejia (2018). The fracture aperture was estimated by

$$b = (3\pi d k_e)^{\frac{1}{3}}, \quad (1)$$

where b is the fracture aperture, d is the diameter of the core, and k_e is the effective oil permeability of the fractured core. Table 3 shows the fracture apertures. The fracture permeability was quantified by

$$k_f = b^2/12. \quad (2)$$

Fracture permeabilities are presented in Table 3.

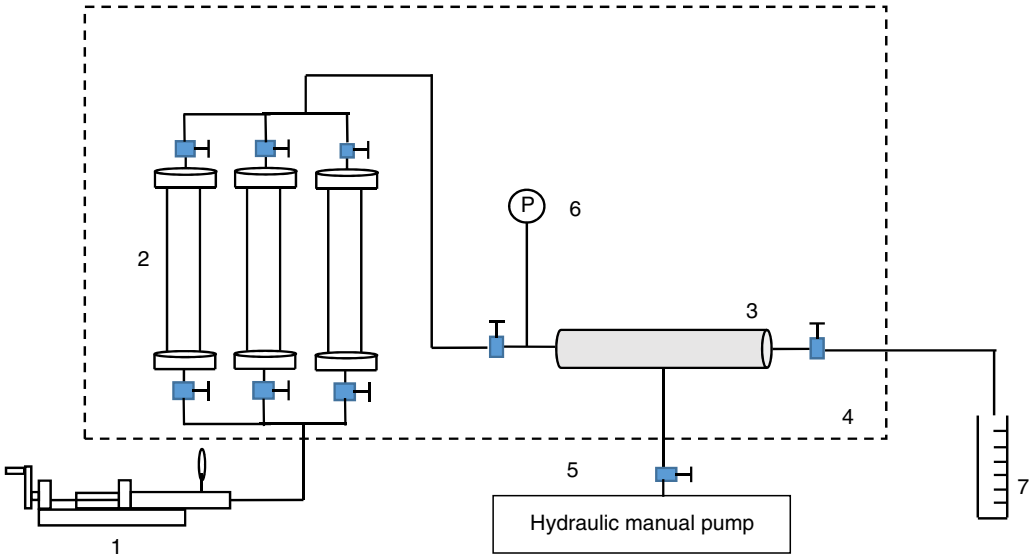

Fig. 3—Schematic of the experimental setup for horizontal dynamic imbibition.

The injection schemes for the four dynamic imbibitions are summarized in **Table 4.** For all cores, the first stage was RB injection at 6 cm^3/h for 1.5 PV injected (PVI), then at 0.05 cm^3/h for 0.3–0.4 PVI, and at 6 cm^3/h until there was no oil production. Then, the second stage was 3pRB injection, for which all cores had a similar residence time of chemical in the fracture (39 minutes). The duration of the second stage (t_2) was designed so that all cores with 3pRB injection had a similar time (corrected by the Leverett factor), $\sqrt{k/\phi}\ t_2$, which is 0.028 ms. Finally, the chase RB was injected at a fixed flow rate until there was no more oil production. For only Core 4, the system was shut in for 20 hours after the 3pRB injection. After that, 3pRB was injected again at 0.51 cm^3/h for 12 days. The outlet of the system was at atmospheric pressure because the experiment used dead crude oil.

	Core 1 (Vertical)	Core 2 (Vertical)	Core 3 (Horizontal)	Core 4 (Horizontal)
First stage	RB was injected at 6 cm^3/h for 1.5 PVI, then at 0.05 cm^3/h for 0.3–0.4 PVI, and at 6 cm^3/h until there was no oil production.			
Second stage	3pRB was injected at 0.6 cm^3/h for 20 hours (1.6 PVI)	Surfactant solution was injected at 0.6 cm^3/h for 25 hours (1.6 PVI)	3pRB was injected at 0.48 cm^3/h for 29 hours (1.3 PVI)	3pRB was injected at 0.51 cm^3/h for 20 hours (0.8 PVI)
Third stage	Chase RB was injected at 0.6 cm^3/h for 19 hours (1.2 PVI)	Chase RB was injected at 0.6 cm^3/h until no oil production	Chase RB was injected at 0.48 cm^3/h until no oil production	Shut in for 20 hours
Fourth stage	–	–	–	3pRB was injected at 0.51 cm^3/h for 12 days (11.3 PVI)

Table 4—Injection schemes during dynamic imbibition with fractured cores.

The produced fluids were received in plastic graduating vials at room temperature. The 3-pentanone concentrations in the produced oleic and aqueous phases were measured using the proton nuclear magnetic resonance method for the chemical slug and chase RB periods for Cores 1, 3, and 4. The 2-EH-4PO-15EO concentration in the produced aqueous phase was measured using the high-performance liquid chromatography method for the chemical slug and chase RB stages of Core 2. The concentration data were used to correct oil-recovery results for 3-pentanone solubility, and to analyze the material balance for each dynamic imbibition.

Material Balance for a Fractured Core. The dynamic imbibition results were analyzed by the material balance for (pseudo)components: brine, oil, and chemical. As mentioned in the Introduction section, the main novelty of this paper lies in this material-balance analysis of fractured coreflooding. The main focus of the analysis is on the following:

- Question 1: What is the fractional amount of the injected component (brine or chemical) that is imbibed into the matrix from the fracture? We would like the injected chemical to be imbibed efficiently into the matrix from the fracture.
- Question 2: What is the relative contribution of brine and chemical to the oil displacement in the matrix PV? Because the chemical is more expensive than brine, we would like brine to displace as much oil in the matrix as possible.

The material balance for (pseudo)component i ($i = 1$ for brine, 2 for oil, and 3 for chemical) for the dynamic imbibition **(Fig. 4a)** is dependent on the following assumptions:

- The system volume consists of two subvolumes: the fracture volume (V_f) and the matrix volume (V_m).
- The fracture volume is connected to the injector (source) and the producer (sink).
- The system is closed except for the injector and producer.
- There is no chemical reaction.

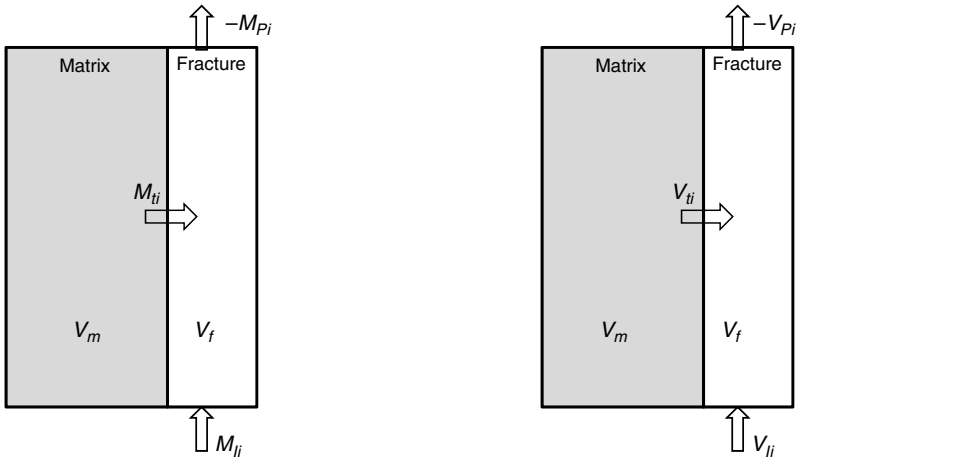

(a) Schematic of dynamic imbibition in terms of mass (b) Schematic of dynamic imbibition in terms of volume

Fig. 4—Schematic of the dynamic imbibition. The system consists of two subvolumes: the fracture and matrix volumes. The fracture volume is connected to the injector (source) and the producer (sink).

For a given time interval Δt,

$$\Delta M_{fi} = M_{ti} + M_{Ii} + M_{Pi}, \quad \ldots\ldots (3)$$

$$\Delta M_{mi} = -M_{ti}, \quad \ldots\ldots (4)$$

where ΔM_{fi} and ΔM_{mi} are the accumulation of component i in the fracture and the matrix, respectively. M_{Ii} is the amount of component i going into the fracture through the injector for Δt, M_{Pi} is the amount of component i going into the fracture through the producer for Δt, and M_{ti} is the amount of component i transferred from the matrix to the fracture through the matrix/fracture interface for Δt.

When this material balance is applied to the time interval Δt, during which flow in the fracture is a (pseudo)steady state, ΔM_{fi} is zero for all i. Then, M_{ti} can be calculated from M_{Ii} and M_{Pi}, which are measurable. How much of the injected amount is actually imbibed into the matrix is quantified by the imbibed fraction for component i (F_i). F_i is defined for Δt as

$$F_i = -M_{ti}/M_{Ii}, \quad \ldots\ldots (5)$$

for $i = 1$ and 3. This imbibed fraction is an "apparent" value because M_{ti} is the net amount of mass transfer from the matrix to the fracture, and because the gross amounts of mass transfer between the matrix and the fracture for Δt are unknown in general.

F_i is related to wettability alteration, but other factors also affect F_i. Among many factors, F_i depends on wettability alteration, the mass transfer of components between the matrix and fracture, and the initial water saturation in the matrix (Argüelles-Vivas et al. 2020).

F_i for surfactant is easy to obtain according to the surfactant amount in the produced aqueous phase measured by the high-performance liquid chromatography method. However, F_i for 3-pentanone can be erroneous because part of 3-pentanone might have been vaporized from the effluent sample before the measurement of the 3-pentanone concentration. Therefore, we needed another method to obtain F_3 without using M_{P3}. To this end, the volume balance was useful, as described in Fig. 4b.

Fig. 5 shows the molar volume for 3-pentanone/oil and 3-pentanone/RB mixtures at 347 K and atmospheric pressure. The volume change on mixing of 3-pentanone and RB was found to be –0.39% when the 3-pentanone concentration was at 1.1 wt%; therefore, the ideal mixing is a reasonable assumption for the data analysis in this research. For a given time interval Δt,

$$\Delta V_f = \sum_{i=1}^{3} (V_{ti} + V_{Ii} + V_{Pi}), \quad \ldots\ldots (6)$$

$$\Delta V_m = -\sum_{i=1}^{3} V_{ti}, \quad \ldots\ldots (7)$$

where ΔV_f and ΔV_m are the volume changes in the fracture and matrix subsystems, respectively. V_{Ii} is the volume of component i injected into the fracture for Δt, V_{Pi} is the volume of component i going into the fracture through the producer for Δt, and V_{ti} is the volume of component i transferred from V_m to V_f through the matrix/fracture interface for Δt.

Assuming that a steady state was reached such that the volume change for each component in the fracture had diminished, we have

$$\Delta V_{fi} = 0 = V_{ti} + V_{Ii} + V_{Pi}, \quad \ldots\ldots (8)$$

for $i = 1$, 2, and 3, and

$$\Delta V_m = 0 = -\sum_{i=1}^{3} V_{ti}. \quad \ldots\ldots (9)$$

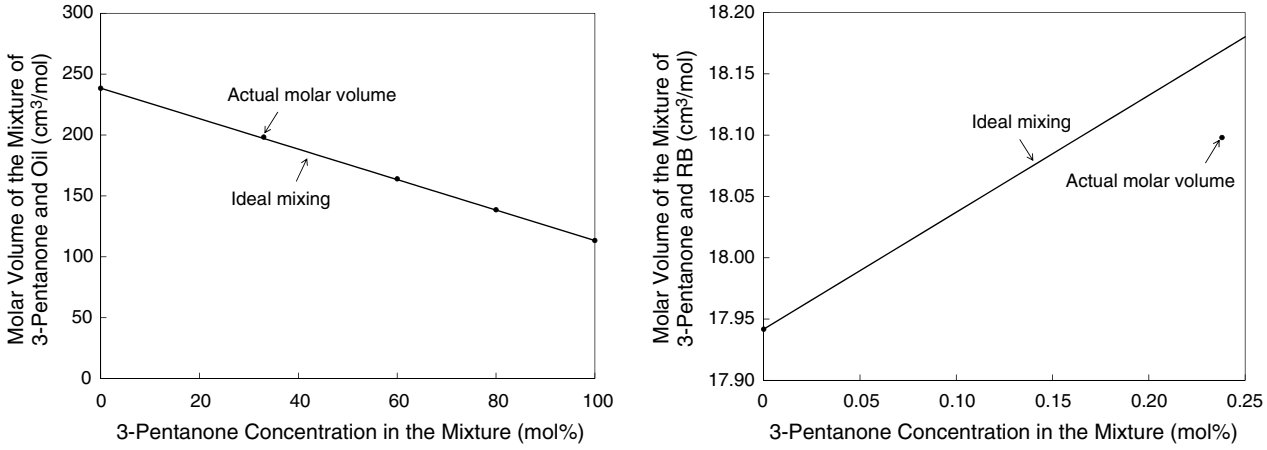

Fig. 5—Molar volume of the mixture of 3-pentanone/oil and 3-pentanone/RB at 347 K and atmospheric pressure.

Then, V_{t3} and F_3 can be expressed in terms of V_I and V_P for the other components as

$$V_{t3} = V_{I1} + V_{P1} + V_{P2}, \quad \ldots\ldots (10)$$

$$F_3 = -V_{t3}/V_{I3} = -(V_{I1} + V_{P1} + V_{P2})/V_{I3}. \quad \ldots\ldots (11)$$

Question 1 given previously in this subsection was addressed by obtaining F_3 by using Eq. 5 for the surfactant case (Core 2) and using Eq. 11 for the 3pRB cases (Cores 1, 3, and 4).

Question 2 was about the contributions of brine ($i = 1$) and 3-pentanone ($i = 3$) to displacing oil ($i = 2$) in the matrix. From Eqs. 8 and 10, the volume of recovered oil can be expressed as

$$V_{P2} = V_{t1} + V_{t3}. \quad \ldots\ldots (12)$$

Therefore, the contribution of component i to displacing oil in the matrix, D_i, is defined as

$$D_i = V_{ti}/V_{P2}, \quad \ldots\ldots (13)$$

for $i = 1$ and 3. Note that $D_1 + D_3 = 1.0$. Eq. 13 was used to address Question 2. We would like D_1 to be higher than D_3 for efficient oil recovery.

The oleic phase saturation in the matrix contained Components 2 and 3 for the 3pRB cases (Cores 1, 3, and 4), and therefore was calculated in two ways,

$$S_{o1} = \frac{OOIM - V_{t2}}{V_m}, \quad \ldots\ldots (14)$$

$$S_{o2} = \frac{OOIM - V_{t2} - V_{t3}}{V_m}, \quad \ldots\ldots (15)$$

where S_{o1} and S_{o2} are the oleic phase saturation, *OOIM* is original oil volume in the matrix, and V_m is the PV of the matrix. The actual saturation of the oleic phase in the matrix should be between S_{o1} and S_{o2} for the 3pRB cases. For dynamic imbibition with a surfactant solution, only S_{o1} was calculated.

Experimental Results

Four dynamic imbibition experiments were presented in this research. The experiment with Core 1 was to quantify the imbibition efficiency of 3-pentanone from a fracture into the surrounding matrix, as well as the relative contribution of brine and 3-pentanone to displacing the oil in the matrix PV. The experiment with Core 2 was to estimate the imbibition efficiency of the surfactant into the matrix from the fracture, and to compare it with the imbibition efficiency of 3-pentanone. The primary purpose of the experiment with Core 3 was to confirm the imbibition efficiency of 3-pentanone that was observed with Core 1. The experiment with Core 4 was to evaluate the potential improvement of the relative contribution of brine to displacing the oil in the matrix by 3pRB injection.

Vertical Dynamic Imbibition with 3pRB (Core 1). Fig. 6 shows the oil recovery for Core 1. Li et al. (2006) showed that, in addition to rock properties, the unit used for oil recovery affected the interpretation of imbibition experiments. Therefore, the oil recoveries in the units of PV and OOIP are presented in Fig. 6. As shown in Table 4, RB was injected into the core until no more oil production was observed. Then, 3pRB was injected to improve the oil recovery for 20 hours. After that, the chase RB was injected for 19 hours. The initial RB injection recovered 13.7% of OOIP (7.0% PV). The incremental oil recovery during the 3pRB injection was 30.9% of OOIP (15.8% PV). The chase-RB injection reached a plateau with an incremental oil recovery of 8.4% of OOIP (4.3% PV). The total oil recovery was 53.0% of OOIP (27.1% PV).

The recovery of oil in the fracture gave the first increase in oil recovery during the RB injection. Then, the oil recovery gradually increased because of brine imbibition. The time scale of this imbibition process is comparable with results in the literature. Li et al. (2017) performed spontaneous-imbibition experiments using Texas Cream Limestone cores of different dimensions. Their samples had similar porosity and permeability as the samples used in this study. They performed brine imbibition in less than 1 day. Mejia (2018) performed seven dynamic imbibition experiments using fractured Texas Cream Limestone cores with the dimensions of 0.037 m in diameter and 0.290 m in length. The periods of the brine injection were shorter than 13 hours for four dynamic imbibition experiments.

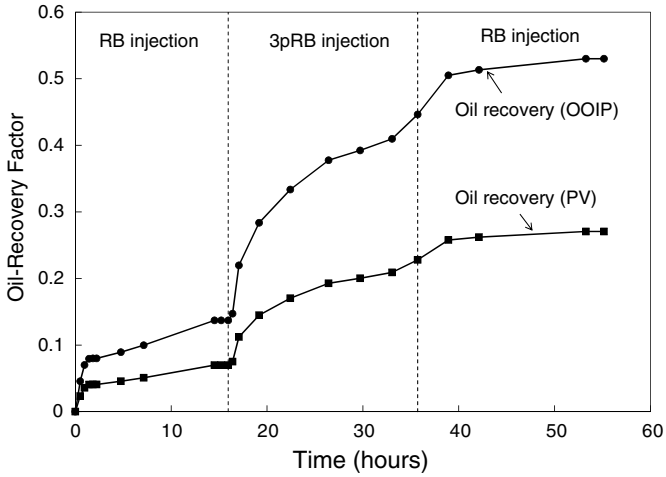

Fig. 6—Oil recovery for Core 1. Oil-recovery curves are given in the units of OOIP and PV. The oil-recovery factor is given as a fraction.

Fig. 7 presents F_1, F_3, S_{o1}, and S_{o2}. The calculation of F_i was performed separately for the three stages (e.g., the time interval for F_i for the 3pRB stage starts after the beginning of the 3pRB injection). S_{o1} and S_{o2} were calculated on a cumulative basis, for which the time interval started at zero across all three stages. The calculations of F_i and S_o for the other cores also follow the same procedure (discussed in the following subsections).

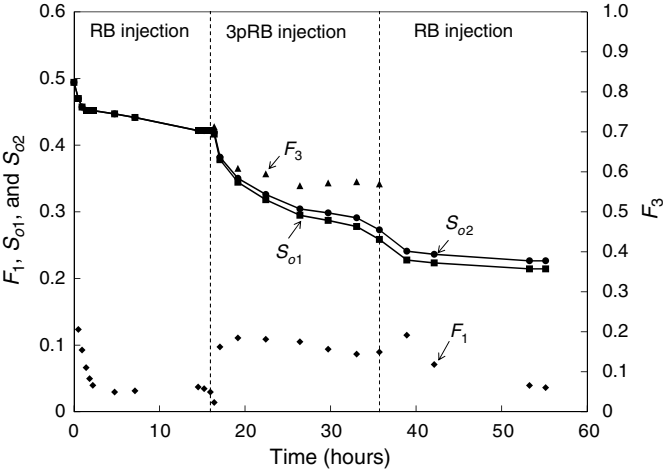

Fig. 7—F_1, F_3, S_{o1}, and S_{o2} for Core 1. The F_3 value after the 3pRB injection was 0.570, indicating that 3-pentanone was imbibed efficiently from the fracture into the matrix. The F_1 value after the 3pRB injection was 0.090, indicating that brine imbibition was enhanced after the wettability alteration by 3-pentanone.

Fig. 8 presents the oil recovery with respect to M_{I3}. M_{I3} was calculated on a cumulative basis, for which the time interval started at the beginning of 3pRB injection. The same procedure was used for the other cores, which will be presented in the following subsections.

Fig. 9 shows $-V_{P2}$ and $-V_{ti}$ for $i = 1$ and 3. These parameters were calculated on a cumulative basis, for which the time interval started at zero across all three stages. D_i was also calculated on a cumulative basis, for which the time interval started after the beginning of the 3pRB injection. This calculation procedure is also applied to the other cores. The results are discussed in the section Discussion.

Vertical Dynamic Imbibition with Surfactant Solution (Core 2). **Fig. 10** shows the oil recovery for Core 2. The initial RB injection recovered 17.3% of OOIP (7.3% PV). The incremental oil recovery during the surfactant-solution injection was 23.6% of OOIP (10.0% PV). The chase-RB injection reached a plateau with an incremental oil recovery of 23.7% of OOIP (10.0% PV). The total oil recovery was 64.6% of OOIP (27.3% PV). Comparison between Figs. 6 and 10 indicates that the final oil-recovery factors given in PV were nearly the same for Cores 1 and 2.

The surfactant-solution injection was stopped before reaching a near-steady state for several reasons. First, we studied the effect of chase-brine injection on oil recovery and mass transfer. Second, we compared all cases on the same basis; for example, the periods of the second stage for Cores 1 and 2 were both 1.6 PVI. Third, we tested the use of a limited amount of the surfactant.

Fig. 11 shows the F_1, F_3, and S_{o1} values from the material balance. **Fig. 12** presents the oil recovery with respect to M_{I3}. **Fig. 13** presents $-V_{P2}$ and $-V_{t1}$. As expected, the values of $-V_{P2}$ and $-V_{t1}$ are close to each other, indicating that the oil was recovered by the displacement by brine, not by the surfactant. That is, the surfactant acted as the wettability modifier, rather than displacing oil by itself. The comparison between the surfactant case with the 3-pentanone case (Core 1) is presented in the section Discussion.

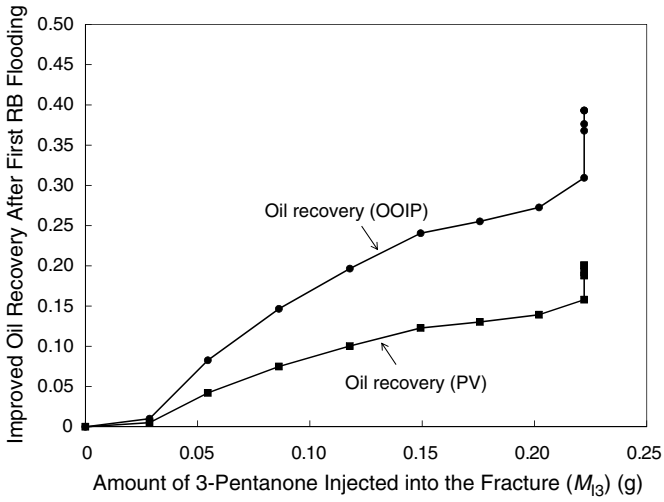

Fig. 8—Oil recovery with respect to the amount of 3-pentanone injected into the fracture for Core 1. The improved oil recovery is given as a fraction.

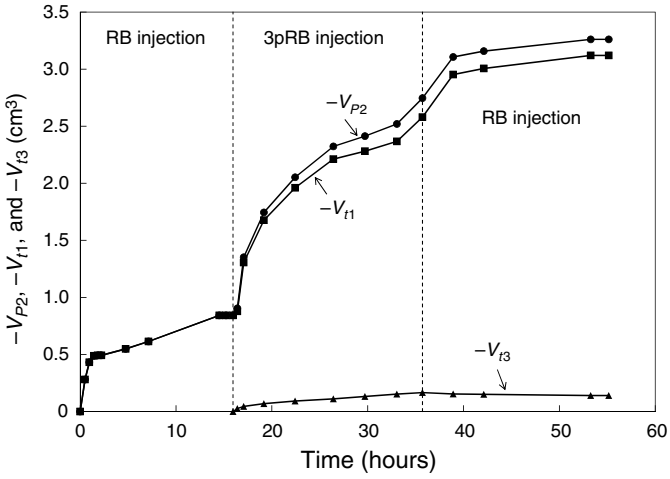

Fig. 9—Values of $-V_{P2}$, $-V_{t1}$, and $-V_{t3}$ for Core 1. During 3pRB injection, the oil was recovered mainly by the displacement by brine.

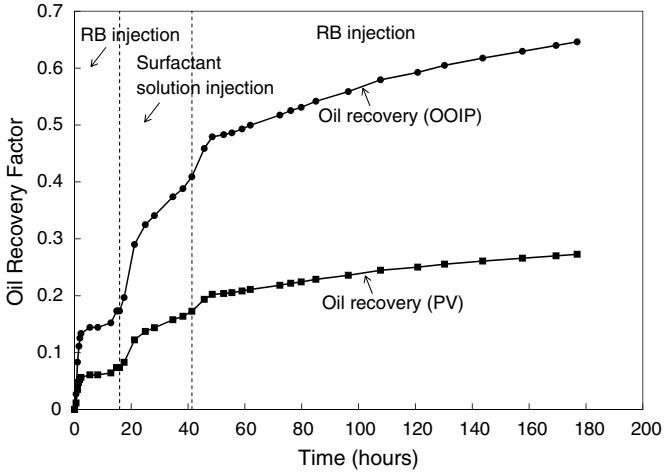

Fig. 10—Oil recovery of Core 2. Oil-recovery curves are given in the units of OOIP and PV. The oil-recovery factor is given as a fraction.

Horizontal Dynamic Imbibition with 3pRB with No Shut-In Period (Core 3). Fig. 14 presents the oil recovery for Core 3. As shown in Table 4, RB was injected into the core until no more oil production was observed. Then, 3pRB was injected to improve the oil recovery for 29 hours. After that, the chase RB was injected until the oil cut became undetectable. The initial RB injection recovered 5.4% of OOIP (2.6% PV). The incremental oil recovery during the 3pRB injection was 7.2% of OOIP (3.4% PV). The chase-RB

injection reached a plateau with an incremental oil recovery of 1.5% of OOIP (0.7% PV). The total oil recovery was 14.2% of OOIP (6.7% PV). It is clear that 3pRB increased oil recovery beyond what the RB injection could recover. **Fig. 15** presents F_1, F_3, S_{o1}, and S_{o2}. **Fig. 16** presents the oil recovery with respect to M_{I3}. **Fig. 17** shows $-V_{P2}$ and $-V_{ti}$ for $i = 1$ and 3.

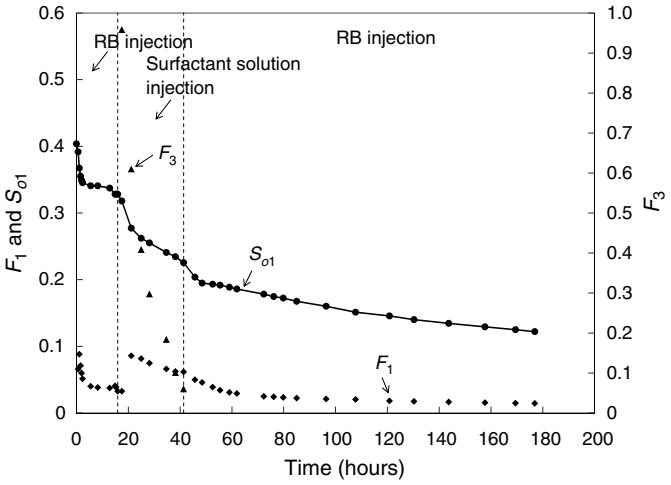

Fig. 11—F_1, F_3, and S_{o1} for Core 2. F_3 was initially large but rapidly decreased to 0.060 at the end of the surfactant-solution injection. The surfactant was less efficient in imbibing into the matrix than 3-pentanone. F_1 was 0.062 at the end of the surfactant-solution injection, indicating that brine imbibition was enhanced after the wettability alteration by the surfactant.

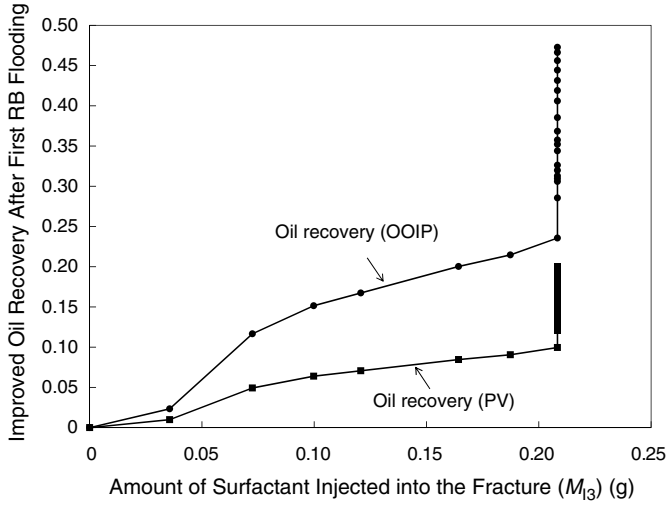

Fig. 12—Oil recovery with respect to the amount of surfactant injected into the fracture for Core 2. The improved oil recovery is given as a fraction.

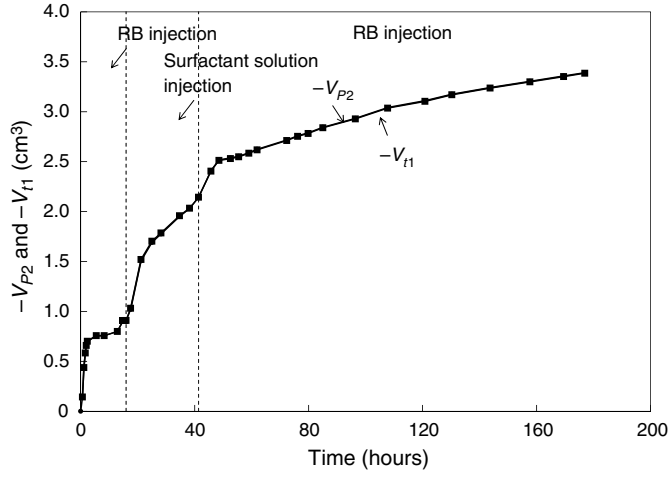

Fig. 13—Values of $-V_{P2}$ and $-V_{t1}$ for Core 2. The values of V_{P2} and $-V_{t1}$ were close to each other, indicating that the oil was recovered essentially by the displacement by brine, not by the surfactant. That is, the surfactant acted as the wettability modifier, rather than displacing oil by itself.

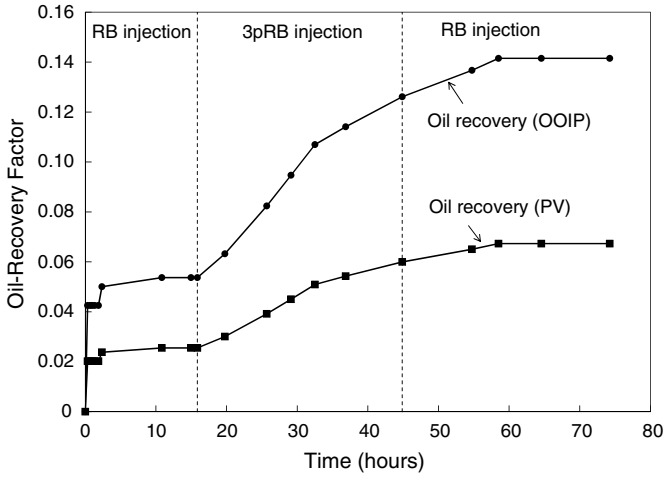

Fig. 14—Oil recovery of Core 3. Oil-recovery curves are given in the units of OOIP and PV. The oil-recovery factor is given as a fraction.

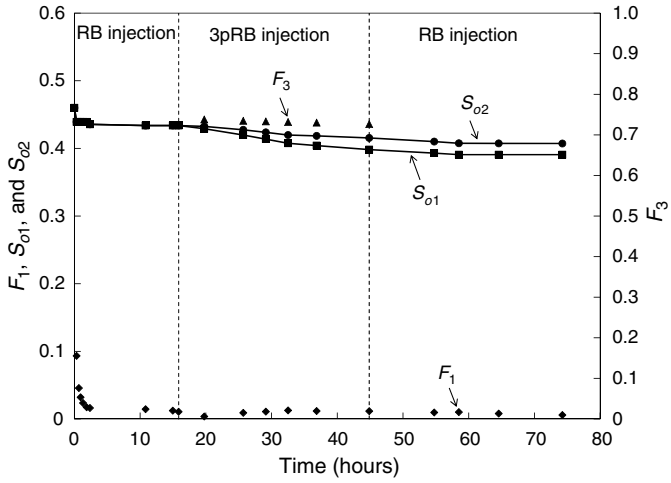

Fig. 15—F_1, F_3, S_{o1}, and S_{o2} for Core 3. The F_3 value after the 3pRB injection was 0.727, indicating that 3-pentanone was imbibed efficiently from the fracture into the matrix. The F_1 value after the 3pRB injection was 0.012, indicating that brine imbibition was enhanced after the wettability alteration by 3-pentanone.

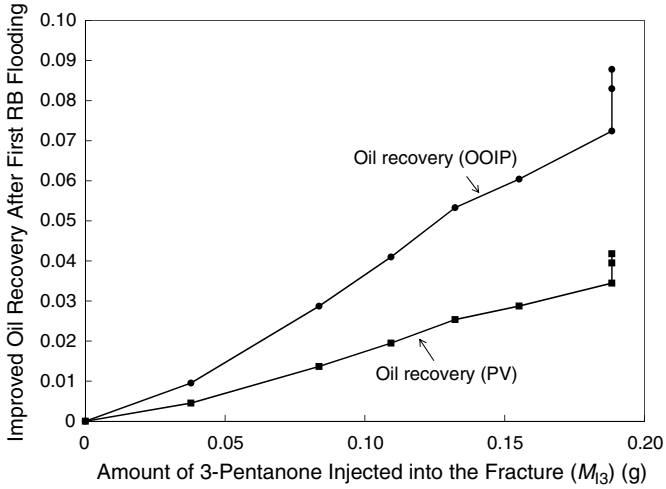

Fig. 16—Oil recovery with respect to the amount of 3-pentanone injected into the fracture for Core 3. The improved oil recovery is given as a fraction.

The oil-recovery factor from Core 1 was greater than that from Core 3. The oleic phase saturation in the matrix at the end of the chase RB was approximately 0.40 for Core 3, which was greater than the final oleic phase saturation for Core 1. Indiana Limestone cores have been reported to be highly heterogeneous (Churcher et al. 1991; Ghosh et al. 2018). The difference observed between Cores 1 and 3 is likely related to their difference in petrophysical properties (Table 3), which affect the initial distribution of the

aqueous and oleic phases. Argüelles-Vivas et al. (2020) showed that 3-pentanone was more effective in enhancing the water imbibition when an aqueous phase was initially present in the matrix. Hence, the effect of 3-pentanone on the enhancement of water imbibition likely depended on the initial distribution of phases in Cores 1 and 3. Table 3 shows that the matrix porosity and permeability of Core 3 were smaller than those of Core 1. A possible scenario is that at the initial oil-wet state, a large fraction of the initial oil in Core 3 resided in smaller pores, while the initial water tended to be in larger pores with oil. The oil produced from Core 3 was mainly from the larger pores where water and oil coexisted, while oil was not efficiently recovered from the smaller pores. In comparison, the initial phase distribution in Core 1 might have been more uniform than that in Core 3, resulting in more-rapid oil recovery from a larger fraction of PV. Also, Cores 1 and 3 were different in terms of flow direction (vertical and horizontal); however, it is unclear how much the small difference in buoyant force between the two cases (compared with the capillary force) contributed to the difference observed in the remaining oleic phase saturation between Cores 1 and 3.

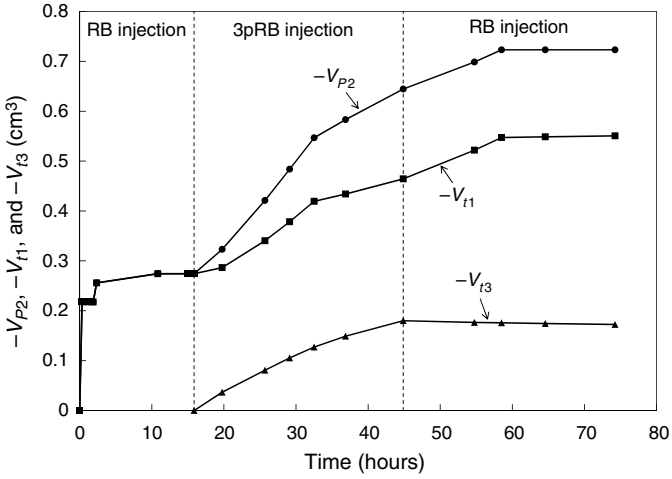

Fig. 17—Values of $-V_{P2}$, $-V_{t1}$, and $-V_{t3}$ for Core 3. During 3pRB injection, brine and 3-pentanone both displaced oil from the matrix PV. Brine and 3-pentanone contributed equally to displacing the oil in the matrix during 3pRB injection.

Horizontal Dynamic Imbibition with 3pRB with a Shut-In Period (Core 4). **Fig. 18** presents the oil recovery for Core 4. RB was injected into the core until no more oil production was observed. Then, 3pRB was injected to improve the oil recovery for 20 hours. After that, the system was shut in for 20 hours. Finally, 3pRB was injected for 12 days. The initial RB injection recovered 8.6% of OOIP (3.4% PV). The incremental oil recovery during the second stage (3pRB injection) was 4.9% of OOIP (2.0% PV). During the shut-in period and subsequent 5-hour 3pRB injection, the incremental oil recovery was 1.8% of OOIP (0.7% PV). During the final stage of 3pRB injection, oil recovery steadily increased by 34.1% of OOIP (13.5% PV). The total oil recovery was 49.5% of OOIP (19.6% PV). It is shown that oil recovery increased during the shut-in period and continued to increase during 12 days of the 3pRB injection. **Fig. 19** shows F_1, F_3, S_{o1}, and S_{o2}. **Fig. 20** presents $-V_{P2}$ and $-V_{ti}$ for $i = 1$ and 3. The detailed analysis of the results is presented in the section Discussion.

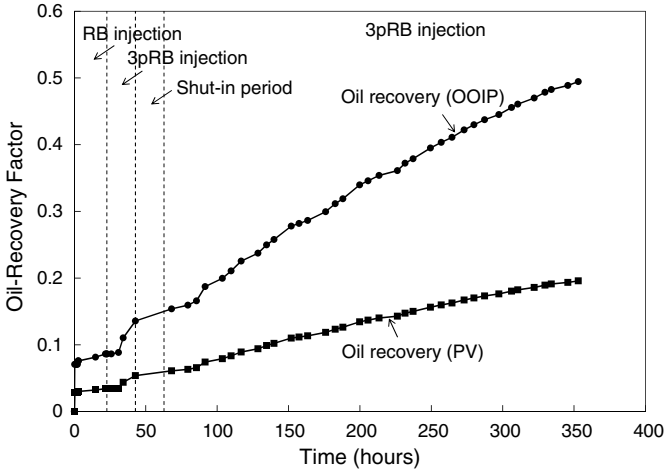

Fig. 18—Oil recovery of Core 4. Oil-recovery curves are given in the units of OOIP and PV. The oil-recovery factor is given as a fraction.

Discussion

The experimental results are discussed through F_1, F_3, and D_1 in this section. F_1 and F_3 represent the imbibed fractions of brine and chemical (3-pentanone for Cores 1, 3, and 4), respectively. D_1 represents the fractional contribution of brine to displacing oil from the matrix.

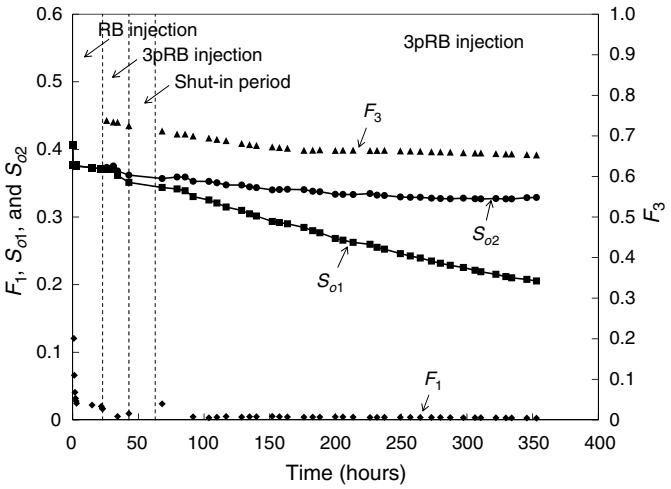

Fig. 19—F_1, F_3, S_{o1}, and S_{o2} for Core 4. F_3 was 0.725 after the second stage (3pRB injection) and was 0.653 after the last stage (3pRB injection), indicating that 3-pentanone was imbibed efficiently from the fracture into the matrix. F_1 was 0.009 after the second stage (3pRB injection). F_1 during the last stage decreased to 0.002 at the end of the last stage.

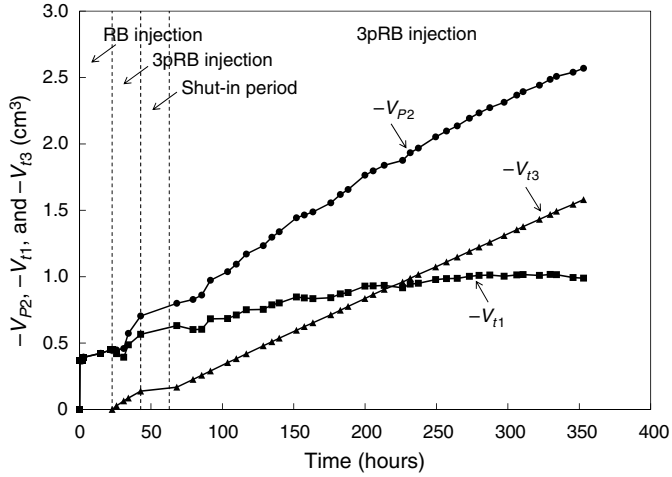

Fig. 20—Values of $-V_{P2}$, $-V_{t1}$, and $-V_{t3}$ for Core 4. During 3pRB injection, brine and 3-pentanone both displaced oil from the matrix PV. The oil recovery occurred mainly because the imbibed 3-pentanone displaced oil in the matrix.

Imbibed Fractions and Fractional Contribution of Brine to Oil Displacement. The F_3 value after the 3pRB injection was 0.570 for Core 1 and 0.727 for Core 3. For Core 4, F_3 was 0.725 after the second stage (3pRB injection) and was 0.653 after the last stage (3pRB injection). These F_3 values indicate that 3-pentanone was imbibed efficiently from the fracture into the matrix. The imbibed fraction of the injected 3-pentanone enhanced the water imbibition by wettability alteration after the initial RB injection reached a plateau in oil recovery. This enhanced water imbibition can be confirmed by the F_1 values: The F_1 value after the 3pRB injection was 0.090 for Core 1 and 0.012 for Core 3. For Core 4, F_1 was 0.009 after the second stage (3pRB injection). F_1 during the last stage decreased to 0.002 at the end of the last stage.

For Core 1, D_1 was 0.913 during the 3pRB injection (i.e., the oil was recovered mainly by the displacement by brine). For Core 3, D_1 was 0.513 during the 3pRB injection [i.e., brine and 3-pentanone (as components) contributed equally to displacing the oil in the matrix]. For Core 4, D_1 was 0.459 during the second stage and 0.202 during the last stage, indicating that the oil recovery occurred mainly because the imbibed 3-pentanone displaced oil in the matrix. The D_1 values for these cases were likely affected by the different petrophysical properties of the cores, as explained in the subsection Horizontal Dynamic Imbibition with 3pRB with no Shut-In Period (Core 3).

Effect of Soaking and Chase Brine on D_1. Because 3-pentanone is more expensive than brine, we would like brine to displace as much oil in the matrix as possible. That is, it is desirable to achieve a higher D_1 value (i.e., a lower D_3 value). The chase-RB stage for Cores 1 and 3 and the shut-in period for Core 4 were designed to evaluate whether such injection schemes increase D_1 (the fractional contribution of brine to the oil displacement in the matrix).

The results from Cores 1 and 3 showed that the chase-RB injection was able to recover oil after the 3pRB injection as long as a sufficient amount of 3-pentanone was imbibed to change the rock wettability. For example, F_1 was 0.036 after the chase-RB injection for Core 1. Fig. 6 shows that the oil-recovery rate decreased rapidly during the chase-RB stage. This is in part because the oleic phase saturation was already small by the end of 3pRB injection (Fig. 7), yielding small capillary forces. Fig. 8 shows that the 3pRB injection made it possible for brine to be imbibed into the matrix even after the initial RB injection established an oil-recovery plateau. Fig. 8 also indicates the importance of optimizing the injection strategy so that the amount of oil produced can be maximized for a given amount of the chemical injected. Such an optimal injection strategy will increase the D_1 parameter (Eq. 13). Similar results were observed for Core 3 (Fig. 16). F_1 during the chase-RB injection was 0.006. Fig. 14 shows that oil recovery quickly reached a plateau during the chase-RB injection.

The results from Cores 1 and 3 demonstrated that D_1 was increased by chase-brine injection. For Core 1, D_1 increased from 0.913 during the 3pRB injection to 0.942 when the 3pRB and chase-RB injection were both considered. Similarly, for Core 3, D_1 was 0.616 when the 3pRB and chase-RB injection were both considered, compared with 0.513 during the 3pRB injection.

The experiment with Core 4 showed that the brine imbibition and oil recovery continued during the shut-in period (without injecting 3pRB), during which the D_1 value increased. During the shut-in period and subsequent 5-hour 3pRB injection, F_1 was 0.024 and D_1 was 0.689. Both are greater than those values at the end of the second stage (F_1 was 0.009 and D_1 was 0.459). Fig. 20 also shows that the rate of brine imbibition was not affected during the shut-in period, but the rate of 3-pentanone imbibition was significantly reduced during the shut-in period. Note that the value of $-V_{t1}$ decreased for some time intervals during the last stage. This is likely because 3-pentanone displaced not only oil, but also brine in the matrix.

Comparison of 3-Pentanone and Surfactant. The results presented in the subsections Vertical Dynamic Imbibition with 3pRB (Core 1) and Vertical Dynamic Imbibition with Surfactant Solution (Core 2) are useful for comparing 3-pentanone with the surfactant as wettability modifiers. F_3 for Core 2 was initially large, but rapidly decreased to 0.060 at the end of the surfactant-solution injection. In comparison, F_3 for Core 1 was 0.570 at the end of the 3pRB stage. A possible reason for the observation is that the surfactant imbibed into the matrix tended to flow back to the fracture more easily than 3-pentanone with Core 1.

The less-efficient imbibition into the matrix can result in less-efficient wettability alteration and brine imbibition by the surfactant. Fig. 11 shows that the imbibed surfactant helped increase F_1 from 0.033 at the end of the initial RB injection to 0.062 at the end of the surfactant-solution injection. In contrast, F_1 was increased from 0.030 at the end of the first RB injection to 0.090 through the imbibition of 3-pentanone into the matrix during the 3pRB injection (Fig. 7). The lower oil-recovery rate for the surfactant case can be caused by both the inefficiency of surfactant imbibition and the lowered IFT between the aqueous phase and the oleic phase (Wang et al. 2019b). These results indicate that an optimal process with a wettability modifier will have a large imbibed fraction to rapidly enhance the oil displacement by brine in the matrix (i.e., large values for F_3 and D_1).

The imbibition of brine into the matrix continued after the surfactant injection was terminated. F_1 was 0.014 after the chase-RB injection. This result confirms that the chase-RB injection continued to recover oil at a small rate (Fig. 10), and is shown in Fig. 12 with respect to M_{I3}. The slow but steady increase in oil recovery by the chase-RB injection might be related to an IFT change during the process because of the following:

- Where the surfactant solution was imbibed, the IFT reduction might make a certain amount of oil mobile, although it also would lower the capillary-driven countercurrent flow of oil and brine.
- The brine/oil IFT would increase after switching to the chase-RB injection, making additional imbibition of brine.

Conclusions

Details of four dynamic imbibition experiments (three with the 3-pentanone solution and one with the surfactant solution) were analyzed by the novel material balance for components: oil, brine, and chemical (either 3-pentanone or surfactant). The analysis resulted in a quantitative evaluation of the imbibed fraction of the components injected (brine and chemical) and the relative contribution of these components to the oil displacement in the matrix. The main conclusions are the following:

1. 3-pentanone was more efficient in transferring from a fracture to the surrounding matrix than 2-EH-4PO-15EO. F_3 was more than 57.0% for 3-pentanone, and only 6.0% for 2-EH-4PO-15EO at the end of the chemical-slug stage.
2. Both 3-pentanone and surfactant enhanced the brine imbibition into the matrix through wettability alteration. For example, F_1 at the end of the 3pRB injection was three times greater than F_1 at the end of the RB injection for Core 1. F_1 at the end of the surfactant-solution injection was two times greater than F_1 at the end of the RB injection for Core 2.
3. During the 3pRB injection stage, brine and 3-pentanone both displaced oil from the matrix PV. Because 3-pentanone is more expensive than brine, it is more advantageous for the imbibed 3-pentanone to enhance the imbibition of brine than to displace oil by itself.
4. Results of the material-balance analysis indicated that an optimal process with a wettability modifier will have a large imbibed fraction (a large F_3) to rapidly enhance the oil displacement by brine in the matrix (for a greater D_1 value). Such a process will benefit from chase-brine injection and soaking (or shut-in) so that the oil recovery could be maximized for a small amount of chemical injection.
5. The chase-RB injection was able to recover oil after the 3pRB injection or surfactant-solution injection as long as a sufficient amount of 3-pentanone/surfactant was imbibed to change the rock wettability.
6. The oil recovery by the brine imbibition continued to occur during the shut-in period after 3pRB injection. The brine-imbibition rate was not affected during the shut-in period, but the rate of oil recovery by the 3-pentanone displacement was significantly reduced during the shut-in period.

Nomenclature

A = cross-sectional area, m^2
b = fracture aperture, m
d = core diameter, m
D = relative contribution of a component to displacing oil in the matrix, dimensionless
F = apparent imbibed fraction, dimensionless
k = permeability, darcies
M = mass, kg
q = injection rate, cm^3/h
S = saturation, dimensionless
t = duration, seconds
V = volume, m^3
τ = residence time, minutes
ϕ = porosity, dimensionless

Subscripts
e = effective
f = fracture

i = index for pseudocomponent
I = injected
m = matrix
o = oleic phase
P = produced
t = transfer

Acknowledgment

Ryosuke Okuno holds the Pioneer Corporation Faculty Fellowship in Petroleum Engineering at the University of Texas at Austin.

References

Abbasi, A. Y., Pope, G. A., and Delshad, M. 2010. Mechanistic Modeling of Chemical Transport in Naturally Fractured Oil Reservoirs. Paper presented at the SPE Improved Oil Recovery Symposium, Tulsa, Oklahoma, USA, 24–28 April. SPE-129661-MS. https://doi.org/10.2118/129661-MS.

Adibhatla, B. and Mohanty, K. K. 2008a. Parametric Analysis of Surfactant-Aided Imbibition in Fractured Carbonates. *J Colloid Interface Sci* **317** (2): 513–522. https://doi.org/10.1016/j.jcis.2007.09.088.

Adibhatla, B. and Mohanty, K. K. 2008b. Oil Recovery from Fractured Carbonates by Surfactant-Aided Gravity Drainage: Laboratory Experiments and Mechanistic Simulations. *SPE Res Eval & Eng* **11** (1): 119–130. SPE-99773-PA. https://doi.org/10.2118/99773-PA.

Allan, J. and Sun, S. Q. 2003. Controls on Recovery Factor in Fractured Reservoirs: Lessons Learned from 100 Fractured Fields. Paper presented at the SPE Annual Technical Conference and Exhibition, Denver, Colorado, USA, 5–8 October. SPE-84590-MS. https://doi.org/10.2118/84590-MS.

Alvarez, J. O. and Schechter, D. S. 2017. Wettability Alteration and Spontaneous Imbibition in Unconventional Liquid Reservoirs by Surfactant Additives. *SPE Res Eval & Eng* **20** (1): 107–117. SPE-177057-PA. https://doi.org/10.2118/177057-PA.

Alvarez, J. O., Neog, A., Jais, A. et al. 2014. Impact of Surfactants for Wettability Alteration in Stimulation Fluids and the Potential for Surfactant EOR in Unconventional Liquid Reservoirs. Paper presented at SPE Unconventional Resources Conference, The Woodlands, Texas, USA, 1–3 April. SPE-169001-MS. https://doi.org/10.2118/169001-MS.

Alvarez, J. O., Tovar, F. D., and Schechter, D. S. 2018a. Improving Oil Recovery in the Wolfcamp Reservoir by Soaking/Flowback Production Schedule with Surfactant Additives. *SPE Res Eval & Eng* **21** (4): 1083–1096. SPE-187483-PA. https://doi.org/10.2118/187483-PA.

Alvarez, J. O., Saputra, I. W. R., and Schechter, D. S. 2018b. The Impact of Surfactant Imbibition and Adsorption for Improving Oil Recovery in the Wolfcamp and Eagle Ford Reservoirs. *SPE J.* **23** (6): 2103–2117. SPE-187176-PA. https://doi.org/10.2118/187176-PA.

Argüelles-Vivas, F. J., Wang, M., Abeykoon, G. A. et al. 2020. Oil Recovery from Fractured Porous Media with/without Initial Water Saturation by Using 3-Pentanone and Its Aqueous Solution. *Fuel* **276** (15 September): 118031. https://doi.org/10.1016/j.fuel.2020.118031.

Austad, T. and Milter, J. 1997. Spontaneous Imbibition of Water into Low Permeable Chalk at Different Wettabilities Using Surfactants. Paper presented at the International Symposium on Oilfield Chemistry, Houston, Texas, USA, 18–21 February. SPE-37236-MS. https://doi.org/10.2118/37236-MS.

Austad, T., Strand, S., Madland, M. V. et al. 2008. Seawater in Chalk: An EOR and Compaction Fluid. *SPE Res Eval & Eng* **11** (4): 648–654. SPE-118431-PA. https://doi.org/10.2118/118431-PA.

Baglai, A. K., Gurarii, L. L., and Kuleshov, G. G. 1988. Physical Properties of Compounds Used in Vitamin Synthesis. *J. Chem. Eng. Data* **33** (4): 512–518. https://doi.org/10.1021/je00054a035.

Bartley, J. P. and Schwede, A. M. 1989. Production of Volatile Compounds in Ripening Kiwi Fruit (Actinidia Chinensis). *J. Agric. Food Chem.* **37** (4): 1023–1025. https://doi.org/10.1021/jf00088a046.

Berlioz, B., Cordella, C., Cavalli, J. et al. 2006. Comparison of the Amounts of Volatile Compounds in French Protected Designation of Origin Virgin Olive Oils. *J. Agric. Food Chem.* **54** (26): 10092–10101. https://doi.org/10.1021/jf061796+.

Bhide, S., Morris, D., Leroux, J. et al. 2003. Characterization of the Viscosity of Blends of Dimethyl Ether with Various Fuels and Additives. *Energy Fuels* **17** (5): 1126–1132. https://doi.org/10.1021/ef030055x.

Boukadi, F. B. H., Watson, R. W., and Owolabi, O. O. 1994. The Influence of Reservoir Rock Properties on Ultimate Oil Recovery in Radial-Core Waterfloods. *J Can Pet Technol* **33** (6): 23–34. PETSOC-94-06-02. https://doi.org/10.2118/94-06-02.

Cavalli, J.-F., Fernandez, X., Lizzani-Cuvelier, L. et al. 2004. Characterization of Volatile Compounds of French and Spanish Virgin Olive Oils by HS-SPME: Identification of Quality-Freshness Markers. *Food Chem* **88** (1): 151–157. https://doi.org/10.1016/j.foodchem.2004.04.003.

Churcher, P. L., French, P. R., Shaw, J. C. et al. 1991. Rock Properties of Berea Sandstone, Baker Dolomite, and Indiana Limestone. Paper presented at SPE International Symposium on Oilfield Chemistry, Anaheim, California, USA, 20–22 February. SPE-21044-MS. https://doi.org/10.2118/21044-MS.

Daubert, T. E. and Danner, R. P. 1985. *Data Compilation Tables of Properties of Pure Compounds.* New York, New York, USA: American Institute of Chemical Engineers.

Ghosh, P. and Mohanty, K. K. 2019. Study of Surfactant–Polymer Flooding in High-Temperature and High-Salinity Carbonate Rocks. *Energy Fuels* **33** (5): 4130–4145. https://doi.org/10.1021/acs.energyfuels.9b00407.

Ghosh, P., Sharma, H., and Mohanty, K. K. 2018. Development of Surfactant-Polymer SP Processes for High Temperature and High Salinity Carbonate Reservoirs. Paper presented at the SPE Annual Technical Conference and Exhibition, Dallas, Texas, USA, 24–26 September. SPE-191733-MS. https://doi.org/10.2118/191733-MS.

Gupta, R. and Mohanty, K. K. 2010. Temperature Effects on Surfactant-Aided Imbibition into Fractured Carbonates. Paper presented at SPE Annual Technical Conference and Exhibition, Anaheim, California, USA, 11–14 November. SPE-110204-MS. https://doi.org/10.2118/110204-MS.

Gupta, R. and Mohanty, K. K. 2011. Wettability Alteration Mechanism for Oil Recovery from Fractured Carbonate Rocks. *Transp Porous Med* **87** (2): 635–652. https://doi.org/10.1007/s11242-010-9706-5.

Hirasaki, G. and Zhang, D. L. 2004. Surface Chemistry of Oil Recovery from Fractured, Oil-Wet, Carbonate Formations. *SPE J.* **9** (2): 151–162. SPE-88365-PA. https://doi.org/10.2118/88365-PA.

Idstein, H. and Schreier, P. 1985. Volatile Constituents from Guava (Psidium Guajava, L.) Fruit. *J. Agric. Food Chem.* **33** (1): 138–143. https://doi.org/10.1021/jf00061a039.

Li, K., Chow, K., and Horne, R. N. 2006. Influence of Initial Water Saturation on Recovery by Spontaneous Imbibition in Gas/Water/Rock Systems and the Calculation of Relative Permeability. *SPE Res Eval & Eng* **9** (4): 295–301. SPE-99329-PA. https://doi.org/10.2118/99329-PA.

Li, Y., Pope, G. A., Lu, J. et al. 2017. Scaling of Low-Interfacial-Tension Imbibition in Oil-Wet Carbonates. *SPE J.* **22** (5): 1349–1361. SPE-179684-PA. https://doi.org/10.2118/179684-PA.

Lu, Y., Najafabadi, N. F., and Firoozabadi, A. 2019. Effect of Low-Concentration of 1-Pentanol on the Wettability of Petroleum Fluid-Brine Rock Systems. *Langmuir* **35** (12): 4263–4269. https://doi.org/10.1021/acs.langmuir.9b00099.

Mejia, M. 2018. *Experimental Investigation of Surfactant Flooding in Fractured Limestones*. Master's thesis, University of Texas at Austin, Austin, Texas, USA.

Mirzaei, M. and DiCarlo, D. 2013. Imbibition of Anionic Surfactant Solution into Oil-Wet Capillary Tubes. *Transp Porous Med* **99** (1): 37–54. https://doi.org/10.1007/s11242-013-0172-8.

Mirzaei, M., DiCarlo, D. A., and Pope, G. A. 2016. Visualization and Analysis of Surfactant Imbibition into Oil-Wet Fractured Cores. *SPE J*. **21** (1): 101–111. SPE-166129-PA. https://doi.org/10.2118/166129-PA.

Nishimura, O., Yamaguchi, K., Mihara, S. et al. 1989. Volatile Constituents of Guava Fruits (Psidium Guajava L.) and Canned Puree. *J. Agric. Food Chem*. **37** (1): 139–142. https://doi.org/10.1021/jf00085a033.

Parra, J. E., Pope, G. A., Mejia, M. et al. 2016. New Approach for Using Surfactants to Enhance Oil Recovery from Naturally Fractured Oil-Wet Carbonate Reservoirs. Paper presented at the SPE Annual Technical Conference and Exhibition, Dubai, UAE, 26–28 September. SPE-181713-MS. https://doi.org/10.2118/181713-MS.

Pet'ka, J., Leitner, E., and Parameswaran, B. 2012. Musk Strawberries: The Flavour of a Formerly Famous Fruit Reassessed. *Flavour Frag J* **27** (4): 273–279. https://doi.org/10.1002/ffj.3095.

Ramanjappa, T. and Rajagopal, E. 1988. Ultrasonic Behavior of the System Water + 3-Pentanone. *J. Chem. Eng. Data* **33** (4): 482–485. https://doi.org/10.1021/je00054a027.

Roehl, P. O. and Choquette, P. W. eds. 1985. *Carbonate Petroleum Reservoirs*. New York, New York, USA: Springer-Verlag.

Wang, M., Abeykoon, G. A., Argüelles-Vivas, F. J. et al. 2019a. Ketone Solvent as a Wettability Modifier for Improved Oil Recovery from Oil-Wet Porous Media. *Fuel* **258** (15 December): 116195. https://doi.org/10.1016/j.fuel.2019.116195.

Wang, M., Baek, K., Abeykoon, G. A. et al. 2019b. Comparative Study of Ketone and Surfactant for Enhancement of Water Imbibition in Fractured Porous Media. *Energy Fuels* **34** (5): 5159–5167. https://doi.org/10.1021/acs.energyfuels.9b03571.